

This article was downloaded by:

On: 25 January 2011

Access details: *Access Details: Free Access*

Publisher *Taylor & Francis*

Informa Ltd Registered in England and Wales Registered Number: 1072954 Registered office: Mortimer House, 37-41 Mortimer Street, London W1T 3JH, UK



Separation Science and Technology

Publication details, including instructions for authors and subscription information:

<http://www.informaworld.com/smpp/title~content=t713708471>

Fractal Dimension of Particle Aggregates in Magnetic Fields

Ching-Ju Chin^{ab}; Shih-Chien Lu^a; Sotira Yiakoumi^a; Costas Tsouris^c

^a School of Civil and Environmental Engineering, Georgia Institute of Technology, Atlanta, Georgia, USA

^b Graduate Institute of Environmental Engineering, National Central University, Chung-Li City, Taoyuan, Taiwan, ROC

^c Oak Ridge National Laboratory, Oak Ridge, Tennessee, USA

Online publication date: 08 July 2010

To cite this Article Chin, Ching-Ju , Lu, Shih-Chien , Yiakoumi, Sotira and Tsouris, Costas(2004) 'Fractal Dimension of Particle Aggregates in Magnetic Fields', *Separation Science and Technology*, 39: 12, 2839 – 2862

To link to this Article: DOI: 10.1081/SS-200028768

URL: <http://dx.doi.org/10.1081/SS-200028768>

PLEASE SCROLL DOWN FOR ARTICLE

Full terms and conditions of use: <http://www.informaworld.com/terms-and-conditions-of-access.pdf>

This article may be used for research, teaching and private study purposes. Any substantial or systematic reproduction, re-distribution, re-selling, loan or sub-licensing, systematic supply or distribution in any form to anyone is expressly forbidden.

The publisher does not give any warranty express or implied or make any representation that the contents will be complete or accurate or up to date. The accuracy of any instructions, formulae and drug doses should be independently verified with primary sources. The publisher shall not be liable for any loss, actions, claims, proceedings, demand or costs or damages whatsoever or howsoever caused arising directly or indirectly in connection with or arising out of the use of this material.

Fractal Dimension of Particle Aggregates in Magnetic Fields

Ching-Ju Chin,^{1,*,#} Shih-Chien Lu,¹ Sotira Yiacoumi,¹
and Costas Tsouris²

¹School of Civil and Environmental Engineering, Georgia Institute
of Technology, Atlanta, Georgia, USA

²Oak Ridge National Laboratory, Oak Ridge, Tennessee, USA

ABSTRACT

Particle flocculation plays a major role in water treatment processes. In flocculation kinetics models it is usually assumed that spherical particles collide and form spherical aggregates. Real aggregates, however, are of irregular shapes and can be considered as fractal objects. The structure of fractal objects can be described by a fractal dimension number that plays an important role in aggregation kinetics. Two-dimensional computer simulations of particle aggregation are carried out in this work to directly observe the evolution of floc size and to determine their fractal

[#]Current address: Graduate Institute of Environmental Engineering, National Central University, Chung-Li City, Taoyuan, Taiwan 320, ROC.

^{*}Correspondence: Ching-Ju Chin, School of Civil and Environmental Engineering, Georgia Institute of Technology, Atlanta, Georgia 30332-0512, USA; E-mail: cjchin@ncuen.ncu.edu.tw.

2839

DOI: 10.1081/SS-200028768

Copyright © 2004 by Marcel Dekker, Inc.

0149-6395 (Print); 1520-5754 (Online)

www.dekker.com

dimension. The computer program developed in this study simulates random particle motion as well as cluster growth. The simulation results are visualized using Java programming language. The fractal dimension of the simulated clusters is determined based on the linear relationship between log-(mass of clusters) and log-(radius of clusters). Primary forces acting on individual particles, including van der Waals, electrostatic, magnetic dipole, and hydrodynamic interparticle forces, are examined to determine the collision efficiency at different collision angles, as well as the structure of the aggregates. The effect of magnetic dipole forces on the fractal dimension and chain formation is examined. It is shown that when the magnetic dipole force is of the same magnitude as the double-layer force within a narrow range of zeta potential values, one-dimensional or two-dimensional clusters may be obtained.

Key Words: Fractal dimension; Brownian flocculation; Magnetic flocculation; Particle aggregation.

INTRODUCTION

Most of the discussions on the aggregation rate of particles in aqueous suspensions start from the work of Smoluchowski.^[1] Initially, there are primary particles in a system, and after a period of aggregation the system contains aggregates of various sizes while the total number of particles decreases. In order to describe how fast the aggregation of primary particles and aggregates proceeds, the aggregation rate is needed, which is determined by the product of the particle collision frequency and collision efficiency.

Aggregation kinetics models are often based on spherical particles. When two spherical primary particles collide, it is usually assumed that they form another spherical particle. Aggregates in real systems, however, are non-spherical. When two primary particles collide, they form a dumbbell-shaped aggregate.^[2] A third particle can attach in several different ways. In real aggregation processes, aggregates containing thousands of primary particles can arise, and it is impossible to provide a detailed description of their structure. Meakin^[3] suggested that aggregates could be recognized as fractal objects, introducing a convenient method to approximate the structure of the aggregates. The fractal concept introduced by Mandelbrot^[4,5] enables the aggregate structure to be characterized in general terms but still convey useful information. Note that in this study, particle is a general term used to describe primary particles, aggregates, and clusters. Aggregates are used in the discussion of colloidal aggregation and clusters are mainly used in the discussion of the cluster-cluster model.

There are various ways to define the fractal dimension. Usually, a particle aggregation system is described by a lattice model and the structure of

aggregates is illustrated by volume and mass fractal dimensions. Both volume and mass fractal dimensions are power-law relationships between length scale and mass and volume, respectively. The mass fractal dimension is defined by:^[2]

$$M \propto R^{D_f} \quad (1)$$

Here, M , which is also called the mass of a cluster, is the number of sites located within a cluster of radius R and D_f is the mass fractal dimension. Box counting is one of the approaches for determining the fractal dimension. A box of size ε is superimposed on a fractal object. By counting the number of boxes intersected by the fractal object, one can obtain a power law relationship:

$$N_{box}(\varepsilon) \propto \varepsilon^{-D_f} \text{ for } \varepsilon \rightarrow 0 \quad (2)$$

For any system, one has $D_f \leq d$, where d is the embedding dimension (dimension of the embedding Euclidean space; in real systems, usually $d = 3$). Cutting out an m -dimensional slice (cross section) of a D_f -dimensional fractal, which is embedded into a d -dimensional space, usually leads to a $D_f - (d - m)$ dimensional object. The density-density correlation function, $C(r)$, which is related to distance r following a power law relationship, is defined by:^[6]

$$C(r) \sim R^{-(d-D_f)} \quad (3)$$

The growth of aggregates due to Brownian diffusion gives an increasing collision radius and a reduced diffusion coefficient, and these effects tend to cancel out, giving a constant collision rate that is not greatly dependent on aggregate size. The hydrodynamic radius of fractal aggregates, which determines the drag and hence the diffusion coefficient, is likely to be smaller than the outer “capture radius,” corresponding to the physical extent of the aggregate.^[2] For high degrees of aggregation, the ratio of the hydrodynamic radius to the “capture radius” is approximately 0.6,^[7] which indicates that Brownian collisions will occur rather more rapidly than predicted from the rate constant. The fluid flow will flow through the voids of fractal aggregates, and thus the porosity of fractal aggregates will affect their drag and settling velocity. Li and Logan^[8] studied the permeability of fractal aggregates and concluded that the Brinkman and Happel permeability equations give more realistic predictions of the aggregates than the Carmen-Kozeny equation.

For smaller values of fractal dimension, the aggregate size increases faster and can give a dramatic increase in aggregation rate.^[9] An obvious consequence of the fractal nature of aggregates is that the effective aggregate volume will not be conserved as assumed in the derivation of collision

rates. There will be a substantial increase in aggregate volume for typical values of D_f , and this is the reason for the increased collision frequency.

Research on aggregation phenomena increased dramatically since the diffusion-limited aggregation (DLA) model was introduced.^[10] The development of the DLA model was stimulated by the earlier experimental works, which demonstrated that fractal structures could be generated by the aggregation of small metal particles in a dense gas. In the Witten-Sander model, particles are added one at a time and move randomly to a growing aggregate of particles. When the randomly moving particle collides with the aggregate, it sticks with the aggregate. Single-particle addition is not a realistic model since, in many aggregation processes, growth occurs as a result of cluster-cluster encounters. Computer simulations using a Witten-Sander model and experimental studies with a range of model colloids^[11] showed open structures with a fractal dimension of around 1.8.

If particles attach permanently to other particles at first contact, the process is controlled entirely by diffusion, hence diffusion-limited aggregation (DLA). When there is interparticle repulsion, so that the collision efficiency is reduced, aggregation is then said to be reaction-limited and very different aggregate structures can be obtained under these conditions. It was found^[11] that reaction-limited aggregates are more compact than those produced by DLA for the cluster-cluster case. When the collision efficiency is low, particles (or aggregates) need to collide many times before sticking occurs, and thus more opportunities exist to explore other configurations and to achieve some degree of interpenetration.^[2]

Ansell and Dickinson^[12] pointed out that the aggregate structure in two dimensions is sensitive to interparticle forces in the range of particle scale. In addition, a rigid cluster has zero internal degrees of freedom, which means that the monomers inside the cluster have fixed distance from each other. Therefore, the cluster is assumed moving as a rigid single particle in the system after it is formed.

Fractal dimension studies of aggregates in shear-flow regimes were also reported. Wiesner^[13] studied the kinetics of fractal-aggregate formation in rapid mixing conditions and found that a 10% error is introduced in calculating the collision efficiency if the aggregate porosity (i.e., the fractal dimension) is neglected. Jiang and Logan^[9] reported that the effect of fractal dimension on collision frequencies is most apparent in shear flocculation and least significant for Brownian flocculation.

Magnetic colloidal particles such as hematite, siderite, goethite, and magnetite particles in a uniform magnetic field experience a magnetic dipole force in addition to the van der Waals, electrostatic, and hydrodynamic forces. Depending on the direction of the centerline between particles with respect to the magnetic field direction, the magnetic dipole force may be attractive or repulsive.

When the magnetic force dominates other interparticle forces, the particles aggregate in a preferred direction, thereby forming chains. Chain formation of superparamagnetic latex particles in a magnetic field was investigated by Chin et al.^[14] Based on experimental observations, Helgesen et al.^[15] concluded that the fractal dimension of aggregates of diffusing magnetized spheres decreases with increasing magnetic moment. Simulation of a mixture of magnetic and nonmagnetic particles also showed chain formation of clusters.^[16]

The present study extends the work of Tsouris and Scott^[17] to investigate the effects on magnetic dipole forces on the fractal dimension of aggregates. A computer simulation approach has been developed for this purpose. Magnetic dipole, van der Waals, double layer, and hydrodynamic forces are used to calculate the collision efficiency of particles in a reaction-limited aggregation under Brownian diffusion. The attractive and repulsive forces are added to give the total energy of interaction between pairs of particles as a function of separation distance and angle with respect to the direction of the magnetic field. Simple models leading to the formation of fractal structures are considered. The significance of this study is that it investigates the effect of magnetic dipole forces on fractal dimension and the effect of fractal dimension on aggregation kinetics in the case that the magnetic dipole force competes with the double-layer force.

THEORETICAL MODEL DEVELOPMENT

The aggregation frequency F_{ij} of particles under the influence of interaction forces is defined as the product of the collision frequency β_{ij} and the collision efficiency E_{ij} ,^[18]

$$F_{ij} = \beta_{ij}E_{ij} \quad (4)$$

Brownian motion dominates collisions between particles smaller than 1 μm ; therefore, in this study, the particle collisions are predominately due to Brownian diffusion and for dilute suspensions, only binary particle collisions occur. The collision frequency for Brownian diffusion is given by^[18]

$$\beta_{ij} = \frac{2 kT}{3 \mu} \frac{(r_i + r_j)^2}{r_i r_j} n_i n_j \quad (5)$$

where k is the Boltzmann constant, T is the absolute temperature, μ is the viscosity of the fluid, as well as n_i , r_i and n_j , r_j are the number concentrations and radii of particles of class i and j , respectively. The class here implies the number of primary particles comprising the aggregate. We can also speak of i -fold and j -fold aggregates. Equation (5) has the very important feature

that, for particles of approximately equal size, the collision frequency becomes independent of particle size. Physically, this behavior is because the increase in particle size leads to a lower diffusion coefficient but a larger collision radius, and these two effects cancel each other when particles are of nearly the same size. For particles of different size, the collision frequency will always be greater than that for equal-size particles.^[2]

The collision efficiency incorporates the effect of particle interaction forces. If there is strong repulsion between particles, then practically no aggregation occurs and the collision efficiency approaches zero. On the other hand, the collision efficiency could be larger than one if there is an additional attractive force, such as a magnetic force. The collision efficiency can be obtained from the solution of the generalized Smoluchowski Eq. (1) for the diffusing particle under the action of interparticle forces,^[17]

$$E_{ij} = \left[(1 + r_j/r_i) \int_{(1+r_j/r_i)}^{\infty} (D_{\infty}/D_{ij}) \exp(V_A/kT) \frac{ds}{s^2} \right]^{-1} \quad (6)$$

where the interaction potential V_A is the summation of electrostatic, van der Waals, and magnetic potentials $V_A = V_{el} + V_{vdw} + V_{mag}$, D_{∞} is the diffusion coefficient in the absence of any interparticle forces, D_{ij} is the relative diffusion coefficient between particles i and j , and $s = r/r_i$ is a dimensionless separation distance between the particles. The hydrodynamic interaction is incorporated in D_{ij} ,

$$D_{ij} = bkT \quad (7)$$

where b is the relative mobility of particles, a function of particle separation.^[17]

Tsouris and Scott^[17] used a direction-average magnetic potential. In this work, the original expression of the magnetic dipole force^[19] is used, which is a function of the angle (α) between the particle centerline and the direction of the magnetic field:^[20]

$$V_{mag} = \frac{4\pi B^2 r_i^3 \chi_i r_j^3 \chi_j}{9\mu_o \left(s \frac{r_i + r_j}{2}\right)^3} (1 - 3 \cos^2 \alpha) \quad (8)$$

where B is the magnetic field strength, α is the angle between the magnetic field direction and the particle center line (a straight line through the centers of both particles, see Fig. 1), χ_i and χ_j are volumetric magnetic susceptibilities of particles i and j , respectively, and μ_o is the magnetic permeability of vacuum ($\mu_o = 4\pi \times 10^{-7} \text{ VsA}^{-1} \text{ m}^{-1}$). The magnetic field is assumed to be homogeneous in the calculation of magnetic potentials. Equation (8) is a function of distance between particles and angle α , however, the angular motion of particles is not considered here.

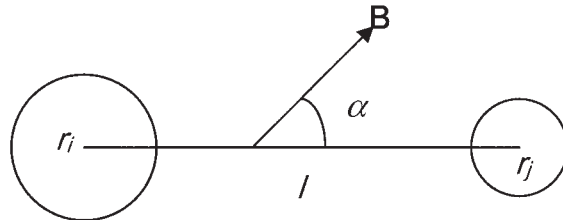


Figure 1. Illustration of particle-centerline and magnetic field direction.

Two different regimes for electrostatic repulsion are used in this study, one for large separations and another for small separations.^[17]

Linear superposition approximation. The linear superposition approximation^[21] is applicable for thin double layers and large interparticle separations:

$$V_{el} = 4\pi\epsilon_r \left(\frac{kT}{e}\right)^2 Y_1 Y_2 \frac{r_i r_j}{l} e^{-\kappa l}, \text{ for } \kappa l \geq 4 \quad (9)$$

where

$$Y_i = 4 \tanh\left(\frac{\Phi_i}{4}\right), \text{ for } \kappa r \geq 10, \Phi_i < 8, \text{ and } i = 1, 2 \quad (10a)$$

$$\Phi_i = \frac{ze\Psi_{oi}}{kT}, \text{ for } i = 1, 2 \quad (10b)$$

$$\kappa \equiv 5.552 \times 10^{-6} \sqrt{I/\epsilon_r kT}, \quad (10c)$$

$$l \cong (s-2) \left(\frac{r_i + r_j}{2} \right). \quad (10d)$$

Here, ϵ_r is the permeability of the medium, e is the electron charge, κ is the inverse of Debye length, z is the valence of the symmetric electrolyte in the solution, l is the shortest separation between two particles, Ψ_{oi} refers to the particle surface potential, and I is the ionic strength of the solution.

Derjaguin approximation. The Derjaguin approximation is used for interparticle dimensionless separations smaller than those at which the linear superposition approximation applies:^[22]

$$V_{el} = \frac{\epsilon_r r_i r_j (\Psi_{oi}^2 + \Psi_{oj}^2)}{4(r_i + r_j)} \times \left[\frac{2\Psi_{oi}\Psi_{oj}}{\Psi_{oi}^2 + \Psi_{oj}^2} \log \left\{ \frac{1 + \exp(-\kappa l)}{1 - \exp(-\kappa l)} \right\} + \log \{1 - \exp(-2\kappa l)\} \right] \quad (11)$$

Because the determination of interparticle forces is based on the actual volume of particles, the magnitude of these forces is assumed independent of the morphology of the aggregates. However, the diffusivity of aggregates is size-dependent; hence, the fractal dimension is required to be included in calculating the diffusivity.

Once the flocculation frequency of particles is obtained as the product of collision frequency and collision efficiency [Eqs. (4)–(6)], a macroscopic population-balance equation can be written to describe the growth of the *i*-fold aggregates. In the absence of aggregate breakup, the discretized form of the population-balance equation is given by

$$\frac{dn_i}{dt} = \frac{1}{2} \sum_{j=1}^{i-1} F_{i(i-j)} n_i n_{(i-j)} - \sum_{j=1}^N F_{ij} n_i n_j \quad (12)$$

where *t* is the time and *N* is the total number of cluster classes in the system. The first term on the right-hand side represents the rate of formation of *i*-fold aggregates by collision of any pair of clusters, *j* and *(i - j)*. Carrying out the summation would mean counting each collision twice and hence the factor 1/2 is included. The second term accounts for the loss of *i*-fold aggregates by collision with any other aggregate or primary particle.

In the population balance equation, Eq. (12), if the radius of a reference aggregate (or particle) is *r*₀ and its volume is *V*₀, for each cluster of radius *r*_{*e*} and volume *V* in the flocculation system, one can write:

$$\frac{r_e}{r_0} = \left(\frac{V}{V_0} \right)^{1/D_f} \quad (13)$$

Reference aggregates are perfect spheres and the mass of cluster in this study is not the conventional mass, therefore the volume (of a reference aggregate or of a fractal cluster) is not directly related to the mass here. From Eq. (13), one can obtain the radius of a cluster as a function of the fractal dimension. By substituting Eq. (13) in the collision frequency, β_{ij} [Eq. (5)], one can introduce the fractal dimension into the aggregation rate and the population balance equation.

The magnetic potential at 0, 45, and 90 degrees between the direction of the magnetic field and the particle-particle centerline is calculated using Eq. (8). The collision efficiency for 0, 45, and 90 degrees can then be obtained from Eq. (6). The collision efficiency is then used to form a sticking probability array in the particle simulation program for the reaction-limited aggregation case.

Java, a modern computer language based on object-oriented programming, was selected for the implementation of particle simulations. It is a full-featured, general-purpose computer language, which has similar syntax

as C and C++. The executable code can be run on various platforms and operating systems.^[23] Since it is a window-based programming language, its visualization capability is suitable for particle simulation. In simulation programs, a class called “particle” is constructed. This particle class is an object that contains the position of particle (or cluster) in simulation space. It also contains attributes of single particle, cluster member, or cluster seed, cluster size, and the number of primary particles in a cluster. This particle class also contains a “move” method and a “paint” method. The move method makes a particle move in the simulated space with a randomly selected direction. The paint method paints the simulation result on the screen when simulation is in progress. The simulation program also generates the average aggregate size and length-mass relationship for fractal dimension calculations.

Particles are first generated at random positions. In this initialization step, two particles should not exist at the same position. If multi-occupation occurs, one of the particles is relocated randomly to an empty lattice site. At this step, the lattice contains a large number of isolated occupied sites and a few small clusters (occupied sites connected by nearest neighbor occupancy).

At each simulation step, particles (or clusters) are selected at random with a probability, which depends on their size in order to represent the effects of a size-dependent diffusion coefficient, and moved by one lattice unit in a randomly selected direction on the lattice. After a particle or cluster has moved, its perimeter is examined to determine whether another object has been contacted (via nearest neighbor occupancy). If another object has been contacted, a new cluster may be formed with the probability given by the sticking probability array. Clusters are formed irreversibly in this model and the sites of a cluster continue to move in the lattice as a single unit. If given a very long simulation time, particles will eventually become one cluster.

There are various ways to determine the fractal dimension of an aggregate; box counting is one of these methods and can be used to determine both computer-simulated and real aggregates. In simulation systems, one can use a log-log relationship to determine fractal dimension. From Eq. (1), $\log M = D_f \log R + c$, where c is a constant. By counting the radius and mass of each particle, the fractal dimension can be obtained from the log-radius vs. log-mass diagram.

Computer simulations can represent fractal phenomena in several ways. Simulation procedures may offer details and insights of real processes and thus assist in interpreting experimental results. During the computer simulation, real-time cluster structures on the screen, as well as distribution of the particle size ratio and fractal dimension, are shown. The modeling program for the solution of the population balance equation was developed by Tsouris and Scott^[17] in FORTRAN. It uses the EPISODE package for solving ordinary differential equations.^[24]

RESULTS AND DISCUSSION

Sticking Probability Array

Collision efficiencies were calculated at a uniform magnetic field from Eqs. (6) and (8) for different conditions that have different magnetic dipole forces. Three collision angles were used to obtain a sticking probability array. Results of collision efficiencies for siderite, hematite, and goethite particles of $0.25\text{ }\mu\text{m}$ diameter at -40 mV zeta potential, 0.1 M NaCl ionic strength, and 0.7 T magnetic field are shown in Table 1. The collision efficiency in the direction parallel to the magnetic field (0 degrees) gives a higher value, and the differences between collision efficiencies at different angles for each species becomes more apparent when the magnetic susceptibility is higher. The collision efficiencies with different collision angles form a sticking probability array. An example of a sticking probability array for magnetic susceptibility = 0.002 is shown in Table 2. In a sticking probability array, a particle (cluster) is located at the center element, four corner elements in the table give the collision efficiency at 45 degrees, elements above and below the particle show the collision efficiency at 0 degree, and elements from the left and the right of the center element represent the collision efficiency at 90 degrees. When two particles collide together, their boundaries are checked with the sticking probability array. If the collision efficiency is greater than one, they will stick together. If the collision efficiency is less or equal than zero, they will not stick together. The collision efficiency between zero and one is used as the probability of sticking in the simulation program.

From Eq. (6), the collision efficiency is a function of the interparticle potential integrated with the distance between the particles. However, the magnetic dipole force is acting not only along the center between

Table 1. Collision efficiencies for different species and collision angles.

Species	Volumetric magnetic susceptibility	Collision efficiency at 0°	Collision efficiency at 45°	Collision efficiency at 90°
Siderite	0.005	2.182	1.245	0
Hematite	0.002	1.077	0.833	0.584
Goethite	0.001	0.833	0.770	0.708

Notes: Ionic strength = 0.1 M , zeta potential = -40 mV , magnetic field strength = 0.7 T , Hamaker constant = $5 \times 10^{-20}\text{ J}$, and $r_i = r_j = 0.25\text{ }\mu\text{m}$.

Table 2. Examples of the sticking probability array.

1.245	2.900	1.245
0	particle	0
1.245	2.900	1.245
0	14.070	0
0	particle	0
0	14.070	0

Notes: Hamaker constant = 5×10^{-20} J, $r_i = r_j = 0.25 \mu\text{m}$, volumetric magnetic susceptibility = 0.002, and zeta potential = -40 mV: (a), magnetic field strength = 1 T, ionic strength = 0.1 M, (b) magnetic field strength = 22.5 T, ionic strength = 0.001 M.

particles but also normal to the centerline. Figure 2 shows the total dimensionless potential, normalized by kT , at different angles α . At $\alpha = 45^\circ$, the magnetic force is still attractive, while at 90° it becomes repulsive (positive).

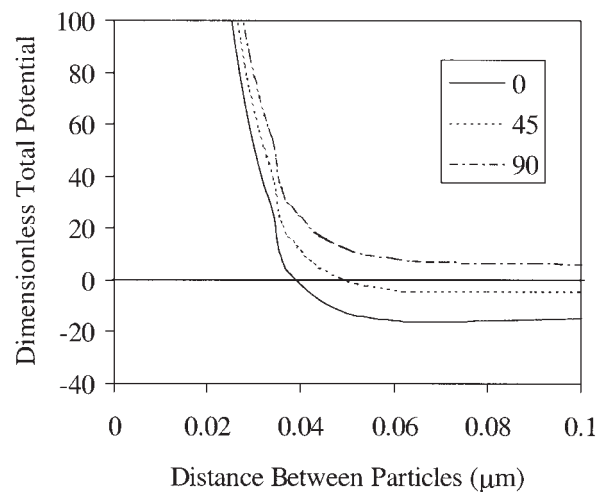


Figure 2. Dimensionless total interparticle potential as a function of the angle between the particle-particle centerline and the magnetic-field direction. (The calculations are not smooth at distances between 0.03 and 0.04 μm because we are assuming two regimes for the electrostatic potential.)

Cluster-Cluster Aggregation Simulation

In the cluster-cluster aggregation model, all clusters are moving randomly with a probability related to their size. When two particles collide, they stick together. Furthermore, when a cluster collides with another cluster, they form a new bigger cluster. Figure 3 shows simulation results of the cluster-cluster aggregation model for a system with no magnetic forces present.

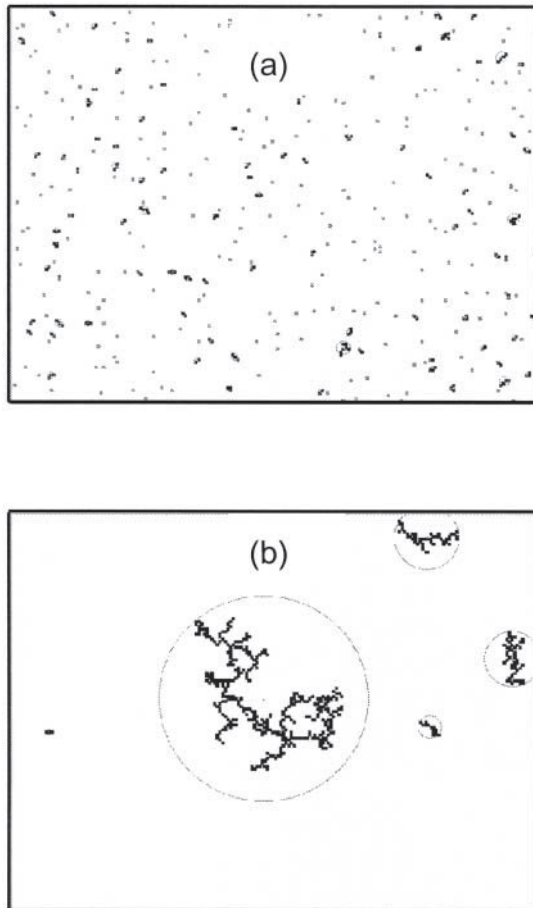


Figure 3. Simulation results using the cluster-cluster aggregation model without magnetic forces; particle number = 475, particle size = 3 pixels: (a) simulation step = 10; (b) simulation step = 1977.

For each cluster, its radius and number of particles inside the radius can be measured. By plotting mass (number of sites occupied within a cluster) vs. radius on a log-log scale, one can obtain the fractal dimension from the slope. When a cluster collides with another cluster, the void space in the new cluster will be bigger than the void space of a cluster colliding with a particle.

Meakin^[3] indicated that if $D_f = d$ (Euclidean dimensionality with a value of 2.0 for 2-D simulation), as clusters grow larger and larger they will approach a constant limiting density. If $D_f < d$, however, the density-density correlation $C(r)$ of the cluster will become smaller and smaller as the cluster grows larger and larger. The simulation results of this work agree with this trend. Figure 4a shows the density-density correlations function of different cluster radii obtained from the simulation. If the density-density correlation is plotted vs. radius on a log-log scale, the slope will be a constant and equal to $(D_f - d)$. Figure 4b shows the log-log result from the simulation. It was found that $(D_f - d) = -0.79$. The theoretical fractal dimension obtained from the density-density function should be around $(2.0 - 0.79) = 1.21$. Figure 4c gives $D_f = 1.21$ using the method of Eq. (1).

Effect of Magnetic Dipole Forces on Fractal Dimension

By comparing the systems with and without magnetic dipole forces, it is found that the fractal dimension is smaller when magnetic dipole forces are present. The magnetic dipole force between particles is attractive along the direction of the magnetic field. Therefore, when the magnetic dipole force is strong enough, it will make particles collide and stick in the direction parallel to that of the magnetic field and form chain-like clusters. The fractal dimension for different magnetic dipole forces was estimated with results shown in Table 3. It was found that the fractal dimension decreases with increasing magnetic susceptibility (or magnetic field).

Results on aggregate morphology are shown in Figs. 5a–c for 0.1 M ionic strength, using the sticking probability arrays listed in Table 4. The aggregates do not have a chain structure, even when the probability of aggregation in the direction normal to the field is zero. The reason for this behavior is that the aggregation probability at 45° is close to 1 as it is at 0°. Thus, the simulation should be extended to account for the tangential magnetic dipole force, which could align the particles in the direction of magnetic field. Moreover, as the particles aggregate, they should be allowed to move around each other for the lowest energy situation. This has not been accounted in the modeling approach so far. However, it can be seen that the clusters are closer to chain-like aggregates at a higher magnetic-field strength.

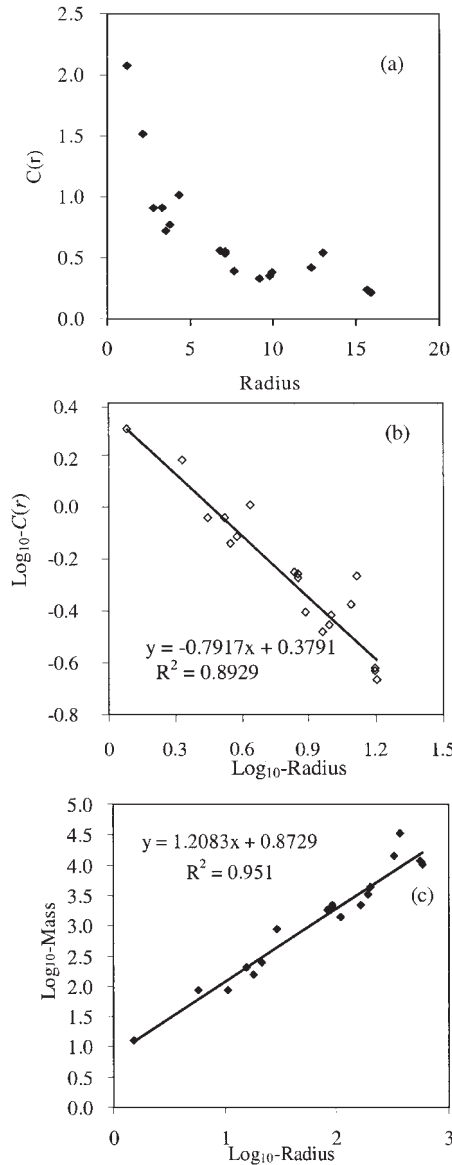


Figure 4. Initial particle number = 600, simulation step = 800, particle size = 3 pixels, Hamaker constant = 5×10^{-20} J, and zeta potential = -60 mV. (a) Density-density correlation function of different cluster radii in cluster-cluster aggregation model; (b) density-density correlation function vs. radius on log-log scale; (c) fractal dimension of clusters.

Table 3. Effect of magnetic dipole forces on fractal dimension.

(a)		Volumetric magnetic susceptibility		
Magnetic field strength (T)		0.005	0.002	0.001
Fractal dimension				
0.1		1.188	1.234	1.246
1		1.219	1.208	1.185
2		1.288	1.198	1.104

(b)		Volumetric magnetic susceptibility		
Magnetic field strength (T)		0.005	0.002	0.001
Fractal dimension				
22.5		1.231	1.326	2.000
25		1.190	1.086	0.908

Notes: Zeta potential = -40 mV , Hamaker constant = $5 \times 10^{-20}\text{ J}$, and $r_i = r_j = 0.25\text{ }\mu\text{m}$: (a) ionic strength = 0.1 M , (b) ionic strength = 0.001 M .

Effect of Fractal Dimension on Collision Efficiency and Collision Frequency

Due to the fractal structure of the aggregates, their hydrodynamic radius is larger than if they were spherical particles. Hence, according to Eqs. (4)–(6), the collision efficiency is different from that of spherical particles. The effect of fractal dimension on the collision frequency and collision efficiency under Brownian diffusion is calculated in Figs. 6a and b vs. the aggregate size ratio of spherical particles. The collision efficiency and collision frequency of the fractal aggregates are normalized to those of ideal spheres. Figure 6a shows that the normalized collision efficiency decreases with increasing fractal dimension of aggregates. In our previous studies,^[25] it was found that the collision efficiency decreases with increasing aggregate size ratio. For fractal objects, the smaller the fractal dimension is, the larger the hydrodynamic radius of the object becomes. Hence, the aggregate size ratio of fractal objects decreases and the difference in the collision efficiency increases as the fractal dimension decreases. In Fig. 6b, it is found that the normalized collision frequency increases rapidly when the fractal dimension is small. This phenomenon occurs

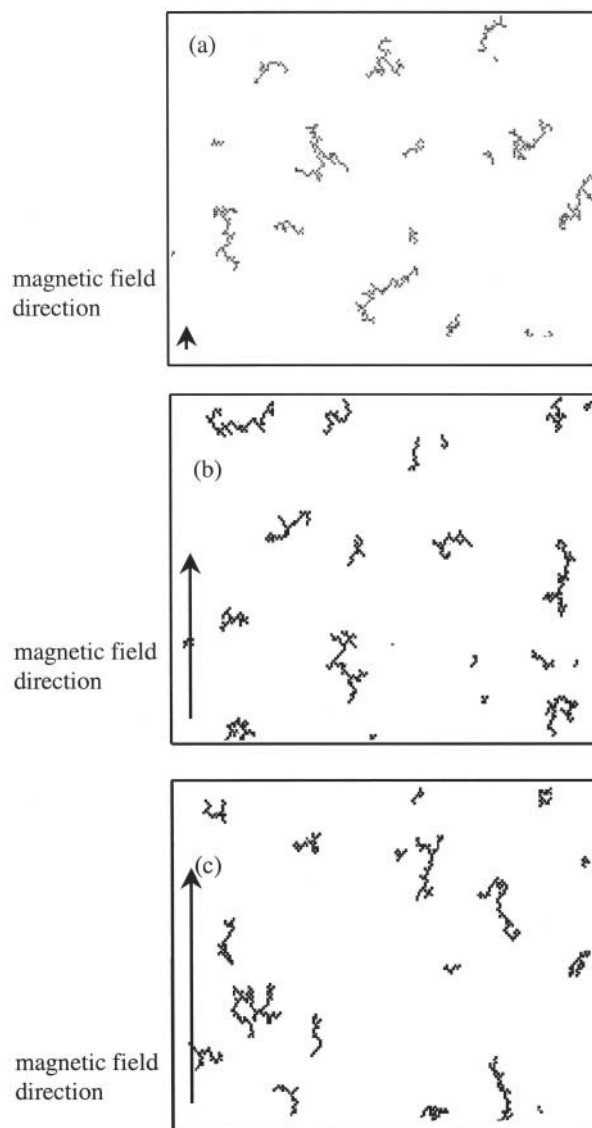


Figure 5. Simulation results showing the effect of field strength on the morphology of aggregates. Arrows indicate the direction of magnetic field and their length are proportional to the strength of the magnetic field. Particle number = 600, simulation step = 800, particle size = 3 pixels, volumetric magnetic susceptibility = 0.002, zeta potential = -60 mV , and Hamaker constant = $5 \times 10^{-20}\text{ J}$. (a) Magnetic field strength = 0.1 T; (b) magnetic field strength = 0.7 T; (c) magnetic field strength = 1 T.

Table 4. Sticking probability array for different magnetic field strength.

(a)		
0.919	1.377	0.919
0	particle	0
0.919	1.377	0.919
(b)		
0.833	1.077	0.833
0.584	particle	0.584
0.833	1.077	0.833
(c)		
0.751	0.756	0.751
0.746	particle	0.746
0.751	0.756	0.751

Notes: Volumetric magnetic susceptibility = 0.002, Hamaker constant = 5×10^{-20} J, zeta potential = -40 mV, ionic strength = 0.1 M, and $r_i = r_j = 0.25 \mu\text{m}$; (a) magnetic field strength = 1 T, (b) magnetic field strength = 0.7 T, (c) magnetic field strength = 0.1 T.

because aggregates of small fractal dimension expand much faster than those of large fractal dimension.

Fractal Dimension as a Function of Simulation Steps

The fractal dimension was calculated every two hundred simulation steps and it was found to increase with the number of steps. After a longer simulation time, the fractal dimension dropped to a steady value (Fig. 7). A stable fractal dimension can be found when there are enough clusters in the system. The fluctuations in the fractal dimension are due to the fact that the number of clusters decreases as the simulation step increases. Spicer et al.^[26] indicated that the fractal dimension increases from 1.1 to 1.4 in shear-induced flocculation for a 6h period. The simulation results of this study are similar to the fractal dimension growth trend in their work.

Influence of Initial Particle Concentration

By varying the initial particle number of the same size particles, it was found that the fractal dimension for varying particle population is different.

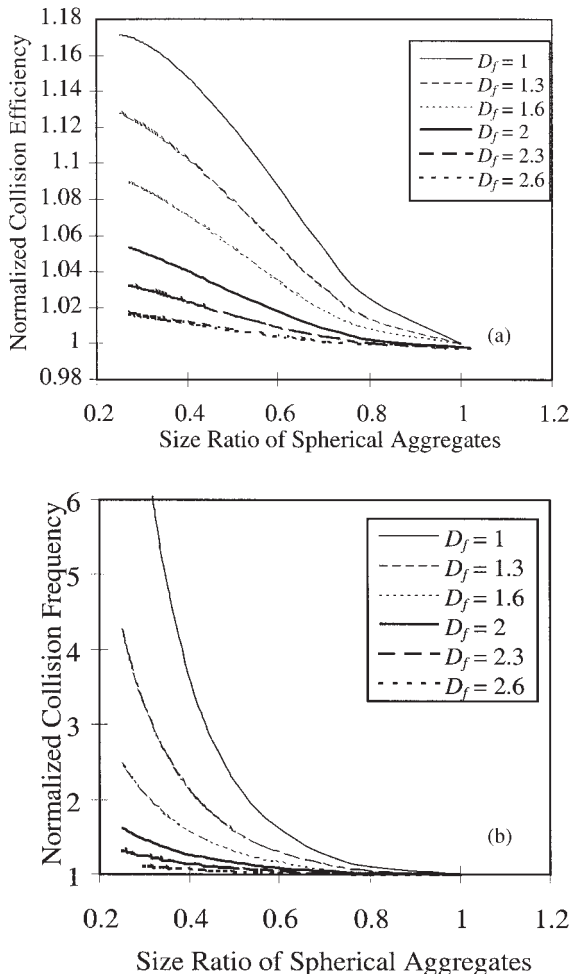


Figure 6. Effect of fractal dimension on (a) collision efficiency normalized to the collision efficiency of spherical aggregates ($D_f = 3$), and on (b) collision frequency normalized to collision frequency of spherical aggregates. Zeta potential = -60 mV, Hamaker constant = 5×10^{-20} J.

The system with a higher initial particle number (or occupied lattice per unit area) will have larger fractal dimension. Figures 4c and 8 show two regression results with different initial particle populations. In Fig. 4c, 600 particles are used in the simulation. After 800 steps, a fractal dimension of 1.28 is obtained. In Fig. 8, 200 particles are used in the system. After 800 steps the fractal

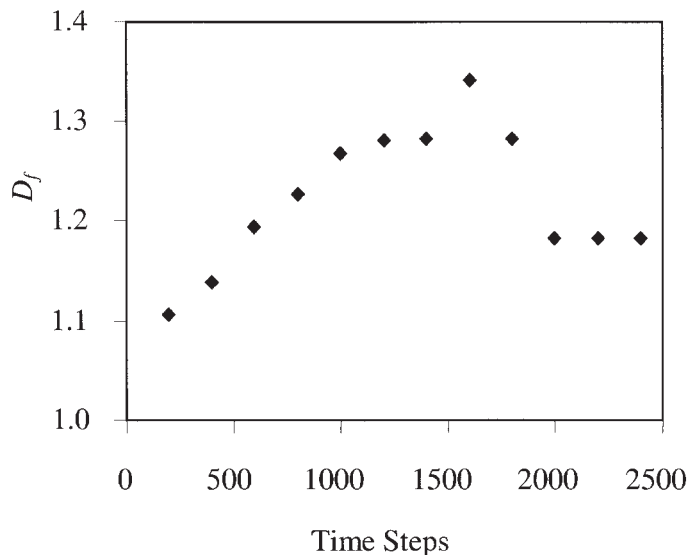


Figure 7. Effect of simulation steps on fractal dimension: particle number = 600, particle size = 3 pixels, zeta potential = -60 mV, volumetric magnetic susceptibility = 0.002, magnetic field strength = 1 T, Hamaker constant = 5×10^{-20} J.

dimension is about 1.038. The reason for this behavior is that for a higher initial concentration, small particles can easily collide into a cluster; thus, the fractal dimension becomes larger.

Meakin^[3] used two different initial particle concentrations (initial particle number per total lattice number) in their simulations. The observed fractal dimension approached a limiting value when initial particle concentration approaches zero. For higher concentration, they obtained a larger fractal dimension. According to Figs. 4c and 8, the simulation results of the present work agree with this conclusion.

Population Balance Equation

There are many input parameters for the population balance equation model, including simulation time, number of volume classes, primary particle size, initial number of particles, particle density and concentration, viscosity, temperature, Hamaker constant, zeta potential, and ionic strength. Figure 9 shows a comparison of the increase in mean aggregate diameter with time for fractal dimensions of 3.0 and 2.4. The experimental values of average

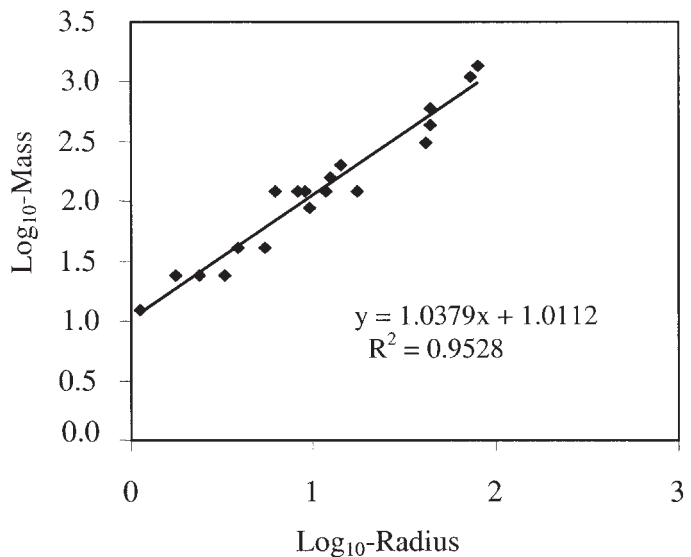


Figure 8. Effect of initial particle number on fractal dimension (in comparison with Fig. 4c): particle number = 200, particle size = 3 pixels, zeta potential = -60 mV, magnetic susceptibility = 0.002, magnetic field strength = 1 T, and Hamaker constant = 5×10^{-20} J.

particle diameter vs. time were obtained from Tsouris and Scott.^[17] A fractal dimension 3.0 (the solid line in Fig. 9) means that we do not consider the fractal dimension effect in the population balance equation. The dashed line is for a fractal dimension of 2.4, which is determined by implementing different values of fractal dimension to the population-balance model to find the best-fit since the cluster-cluster model developed in this work uses a two-dimensional lattice system. With a smaller fractal dimension, aggregates grow faster than with a larger fractal dimension and are closer to the experimental values. Based on the results in Fig. 9, we conclude that the fractal dimension is an important parameter for determining the average size of particle aggregates with time.

SUMMARY AND CONCLUSIONS

Aggregates are often irregular in natural systems and can be treated as fractal objects. A fractal dimension can be used to describe their structure. The fractal dimension was introduced in a population-balance-equation

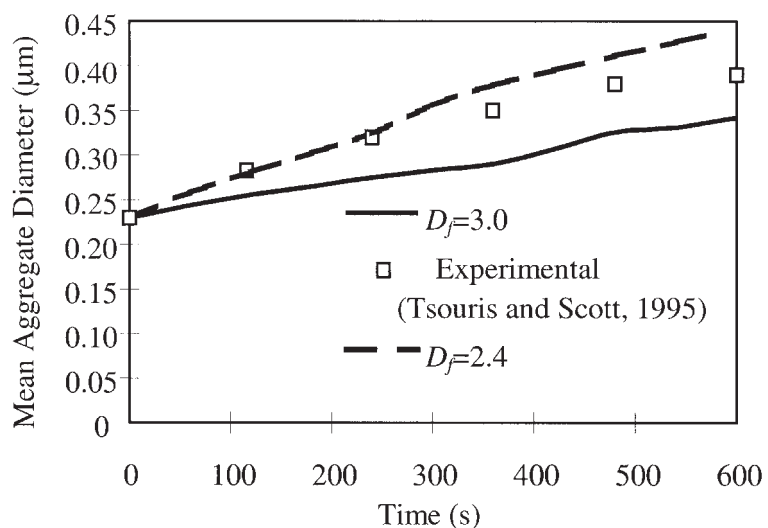


Figure 9. Effect of fractal dimension on the growth of the average particle diameter from the population balance equation. Magnetic field strength = 6 Tesla (T), magnetic susceptibility = 0.002, Hamaker constant = 5×10^{-20} J, zeta potential = -50 mV, and particle concentration = 3.8 mg/L.

model to investigate the effect on the flocculation rate under Brownian diffusion. It was found that the fractal dimension is an important parameter in flocculation kinetics. Systems with a smaller fractal dimension have a higher flocculation rate, and the resulting mean aggregate diameter becomes bigger.

For a self-similar aggregate, a power-law relationship is obtained between radius (length) and mass. Simulation results in this work were in agreement with this power-law relationship. In the cluster-cluster aggregation model, all clusters in the simulation system are selected with a collision probability related to their size. The collision efficiency and frequency become larger after the fractal dimension is considered in the simulation. The fractal dimension was obtained by plotting the relationship between density-density correlation vs. radius of clusters on a log-log scale. The fractal dimension obtained from the cluster-cluster aggregation model is between 1.0 and 1.6 for two-dimensional aggregates. Simulation results also indicate that the morphology of magnetized particles is different in a strong uniform magnetic field. The fractal dimension is smaller when a magnetic force is present, which is due to the chain formation of aggregates. The magnetic susceptibility of the particles and magnetic-field strength were found to be important parameters in this simulation.

NOMENCLATURE

A	Hamaker constant (J)
B	magnetic field strength (T)
b	relative mobility function
$C(r)$	density-density correlation function
d	embedding dimension
D_f	fractal dimension
D_∞	diffusion coefficient in the absence of any interparticle forces ($\text{m}^2 \text{s}^{-1}$)
$D_{ij}^{(0)}$	relative diffusion coefficient ($\text{m}^2 \text{s}^{-1}$)
e	electron charge = $1.6 \times 10^{-19} \text{ C}$
E_{ij}	collision efficiency
F_{ij}	aggregation frequency ($\text{m}^3 \text{s}^{-1}$)
I	ionic strength of the solution (M)
i, j	subscript to indicate the class of a cluster
k	Boltzmann constant = $1.38 \times 10^{-23} \text{ J K}^{-1}$
l	shortest separation between two particles (m)
M	mass of a cluster
N	number of clusters classes in the system
$N_{box}(\varepsilon)$	number of boxes intersected by the fractal object
n_i, n_j	numbers of particles per unit volume in the cluster class i and j
r	distance between particles (m)
R	radius of a cluster (m)
r_i, r_j	particle radii (m)
s	dimensionless distance between two spheres
t	time (s)
T	absolute temperature (K)
V_A	total interparticle potential (V C)
V_{el}	electrostatic potential (V C)
V_{mag}	magnetic potential (V C)
V_{vdw}	van der Waals potential (V C)
α	angle between the particle centerline and the direction of the magnetic field
β_{ij}	collision frequency
χ_i, χ_j	volumetric magnetic susceptibilities of particle i and j
ε	box size that superimposed on the fractal object
ε_r	permeability of medium = $89 \times 10^{-10} (\text{C V}^{-1} \text{ m}^{-1})$ for water
κ	inverse of Debye length (m^{-1})
μ	fluid viscosity ($\text{kg m}^{-1} \text{ s}^{-1}$)
μ_o	magnetic permeability of vacuum ($4\pi \times 10^{-7} \text{ VsA}^{-1} \text{ m}^{-1}$)
Ψ_{oi}	particle surface potential (V)

ACKNOWLEDGMENT

Partial support for this research was provided by the National Science Foundation through a Career Award (BES-9702356 to S.Y.), and by the Division of Chemical Sciences, Office of Basic Energy Sciences, U.S. Department of Energy, under contract DE-AC05-00OR22725 with UT-Battelle, LLC.

REFERENCES

1. Smoluchowski, M. Versuch einer mathematischen Theorie der Koagulationskinetic kolloider Lösungen. *Z. Physik. Chem.* **1917**, *92*, 129–168.
2. Elimelech, M.; Gregory, J.; Jia, X.; Williams, R. *Particle Deposition and Aggregation—Measurement, Modeling and Simulation*; Butterworth Heinemann: Oxford, 1995.
3. Meakin, P. Diffusion-limited aggregation in three dimensions: results from a new cluster–cluster aggregation model. *J. Colloid Interf. Sci.* **1984**, *102*, 505–512.
4. Mandelbrot, B.B. *Fractals: Form, Chance, and Dimension*; Freeman: San Francisco, 1977.
5. Mandelbrot, B.B. *The Fractal Geometry of Nature*; Freeman: San Francisco, 1982.
6. Meakin, P. Simulations of aggregation processes. In *The Fractal Approach to Heterogeneous Chemistry; Surfaces, Colloids, Polymers*; Avnir, D., Ed.; John Wiley & Sons: Chichester, 1989; 131–160.
7. Torres, F.E.; Russel, W.B.; Schowalter, W.R. Floc structure and growth kinetics for rapid shear coagulation of polystyrene colloids. *J. Colloid Interf. Sci.* **1991**, *142*, 554–574.
8. Li, X.; Logan, B.E. Permeability of fractal aggregates. *Wat. Res.* **2001**, *35*, 3373–3380.
9. Jiang, Q.; Logan, B.E. Fractal dimensions of aggregates determined from steady-state size distributions. *Environ. Sci. Tech.* **1991**, *25*, 2031–2038.
10. Witten, T.A.; Sander, L.M. Diffusion-limited aggregation, a kinetic critical phenomenon. *Phys. Rev. Lett.* **1981**, *47*, 1400–1403.
11. Lin, M.Y.; Lindsay, H.M.; Weitz, D.A.; Ball, R.C.; Klein, R.; Meakin, P. Universality in colloid aggregation. *Nature* **1989**, *339*, 360–362.
12. Ansell, G.C.; Dickinson, E. Aggregate structure and coagulation kinetics in a concentrated dispersion of interacting colloidal particles. *Chem. Phys. Lett.* **1985**, *122*, 594–598.
13. Wiesner, M.R. Kinetics of aggregate formation in rapid mix. *Water Res.* **1992**, *26*, 379–387.

14. Chin, C.J.; Yiacoumi, S.; Tsouris, C. Probing DLVO forces using inter-particle magnetic forces: transition from secondary-minimum to primary-minimum aggregation. *Langmuir* **2001**, *17*, 6065–6071.
15. Helgesen, G.; Skjeitorp, A.T.; Mors, P.M.; Botet, R.; Jullien, R. Aggregation of magnetic microspheres: experiments and simulations. *Phys. Rev. Lett.* **1988**, *61*, 1737–1739.
16. Trohidou, K.N.; Blackman, J.A. Aggregation and segregation in a mixture of magnetic and nonmagnetic particles. *Phys. Rev. B* **1995**, *51*, 11521–11526.
17. Tsouris, C.; Scott, T.C. Flocculation of paramagnetic particles in a magnetic field. *J. Colloid Interf. Sci.* **1995**, *171*, 319–330.
18. Valioulis, I.A.; List, E.J. Collision efficiency of diffusing spherical particles: hydrodynamic, van der Waals and electrostatic forces. *Adv. Colloid Interf. Sci.* **1984**, *20*, 1–20.
19. Chikazumi, S. *Physics of Magnetism*; Wiley: New York, 1964.
20. Yiacoumi, S.; Rountree, D.A.; Tsouris, C. Mechanism of particle flocculation by magnetic seeding. *J. Colloid Interf. Sci.* **1996**, *184*, 477–488.
21. Bell, G.M.; Levine, S.; McCartney, L.N. Approximate methods of determining the double-layer free energy of interaction between two charged colloidal spheres. *J. Colloid Interf. Sci.* **1980**, *33*, 335–360.
22. Hogg, R.; Healy, T.W.; Fuerstenau, D.W. Mutual coagulation of colloidal dispersions. *Trans. Faraday Soc.* **1966**, *18*, 1638–1651.
23. Flanagan, D. *Java in a Nutshell*; O'Reilly & Associates Inc: Sebastopol, 1996.
24. Hindmarch, A.C.; Byrne, G.D. *EPISODE: An Effective Package for the Integration of System of Ordinary Differential Equations*; 1976; Lawrence Livermore Laboratory Report UCID-30112.
25. Chin, C.J.; Yiacoumi, S.; Tsouris, C. Shear-induced flocculation of colloidal particles in stirred tanks. *J. Colloidal Interf. Sci.* **1998**, *206*, 532–545.
26. Spicer, P.T.; Keller, W.; Pratsinis, S.E. The effect of impeller type on floc size and structure during shear-induced flocculation. *J. Colloid Interf. Sci.* **1996**, *184*, 112–122.